4B.5 NUMERICAL SIMULATIONS OF LEAD-GENERATED CLOUDS AND THEIR EFFECT ON LARGE-SCALE SURFACE FLUXES

Michael A. Zulauf * and Steven K. Krueger
University of Utah, Salt Lake City, Utah

1. INTRODUCTION

Due to the extreme temperature differences between the air and the sea surface during the Arctic winter, leads can be a significant source of heat and moisture for the Arctic atmosphere. Because of their relatively small scales, these quasi-linear openings in the pack ice can not be explicitly resolved by large-scale models.

Despite this fact, such small-scale features may in fact have significant impacts upon the large-scale atmosphere. For example, while leads typically account for only 1 – 2% of the surface area of the Arctic, the surface fluxes of heat and moisture from them may be in excess of two orders of magnitude greater than those through the ice and snow surface. Thus, the total fluxes associated with leads can be of the same magnitude as those through the ice and snow surfaces.

In addition, the convective plumes emanating from leads have been observed to contribute to cloud development under certain conditions. As seen at the Surface Heat Budget of the Arctic Ocean (SHEBA) site, the presence of clouds can profoundly impact the energy balance at the surface through radiative effects. Depending upon lead size and ambient atmospheric conditions, the convective plumes, and associated cloud development, may penetrate to varying depths, and thus have a variable impact upon the surface fluxes.

Previous studies have investigated the local dynamics of plume development, or the extent and height which the plumes can attain. For example, Glendening (1994) examined the impact of orientation of the large-scale wind field over a 200 m wide lead. Pinto and Curry (1997) studied the effects of radiation and microphysics on plume development over wide leads using a one-dimensional model. And Burk et al. (1997) examined the development of plumes under realistic conditions. Despite these and other studies, there has been relatively little investigation into the impacts of leads on the large-scale heat and moisture budgets.

In an attempt to better understand the effects the enhanced small-scale surface fluxes can have upon the large-scale, the two-dimensional cloud resolving model (CRM) of Krueger et al. (1995) is employed here. Numerous observations from the SHEBA project have been used as the basis for an idealized clear-sky mid-winter case, and the various feedbacks which affect the surface-energy budget are investigated.

* *Corresponding author address:* Michael A. Zulauf
Department of Meteorology, University of Utah, Salt Lake City, UT 84112. e-mail: mazulauf@met.utah.edu

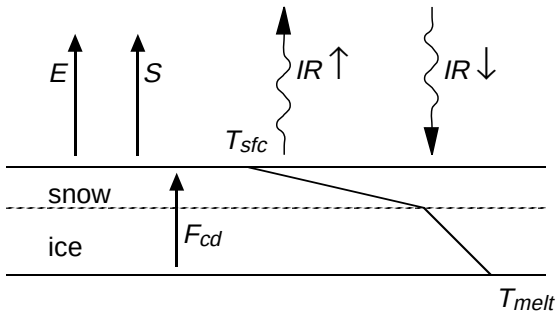

Figure 1: Conductive heat flux at surface is calculated using the internal ice/snow temperature profile, which is integrated in time using the one-dimensional heat equation.

2. THE SURFACE HEAT BUDGET

In order to accurately model the surface heat budget over a wide domain, it is necessary to handle the surface temperature in a more realistic fashion than has been commonly used for these types of simulations, namely holding the temperature of the snow/ice surface constant. Instead, the CRM has been modified to calculate the conductive heat flux through the ice/snow layers, and T_{sfc} is diagnosed to satisfy an energy balance at the surface,

$$F_{cd} = (IR\uparrow - IR\downarrow) + S + E \qquad (1)$$

where F_{cd} is the conductive heat flux, $IR\uparrow$ and $IR\downarrow$ are the upwards and downwards longwave fluxes, S is the sensible heat flux, and E is the latent heat flux. The conductive heat flux at the surface is calculated using the internal ice/snow temperature profile, which is integrated in time using the one-dimensional heat equation. This method is similar to that used by Ebert and Curry (1993), and is displayed schematically in Figure 1.

An additional benefit of this approach is that it allows for the easy investigation of the effects of the refreezing process. While we do not yet explicitly simulate refreezing, we can examine the effects of a thin ice layer upon the surface energy budget. Figure 2 displays

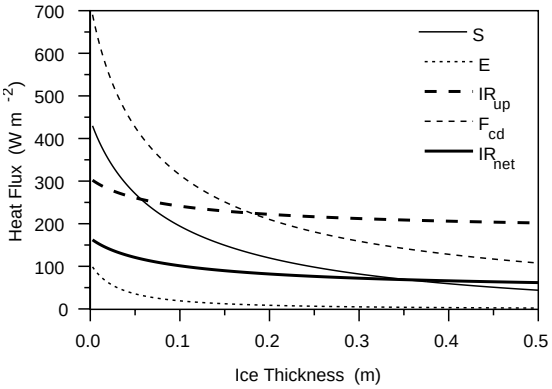

Figure 2: Surface fluxes over partially refrozen leads, as a function of ice thickness.

the surface fluxes above a surface of ice of variable thickness. The ambient conditions used in calculating this balance are $IR\downarrow = 140$ W m^{-2}, $T_{air} = 240$ K, $RH = 80\%$ with respect to liquid water, a 10-m wind speed of 5 m s^{-1}, and a surface roughness of 0.2 mm.

3. CONDITIONS AT SHEBA

In the process of initializing simulations that represent typical conditions at the SHEBA site, observational data from a number of sources was examined. Atmospheric soundings from rawinsondes (Moritz, 1999) were examined for the month of January, 1998, and typical clear-sky conditions were noted. Figure 3 displays the air temperature and wind speed observed on January 18, 1998, which was found to be typical of this time period. The CRM was then initialized based on idealized versions of these soundings (as well as profiles of RH and wind direction).

To determine the location and size of active leads, synthetic aperture radar (SAR) imagery from the Canadian RADARSAT satellite was examined (Stern, 1999). In Figure 4, which displays an image from January 20, 1998, a large lead is seen to the east of the SHEBA site. By comparisons with SAR imagery from three days prior, and by examining NOAA high resolution satellite IR imagery (not shown), it is clear that this is indeed an active, newly opened lead. Furthermore, the data from the rawinsondes, as well as that from PAM stations, etc. show that the predominant large-scale wind is from a northeasterly direction, crossing the large lead (and others nearby) nearly perpendicularly prior to reaching the SHEBA site.

With conditions such as these, it would be expected to see some signature of the large lead and associated convective plumes in the observations at the ice camp.

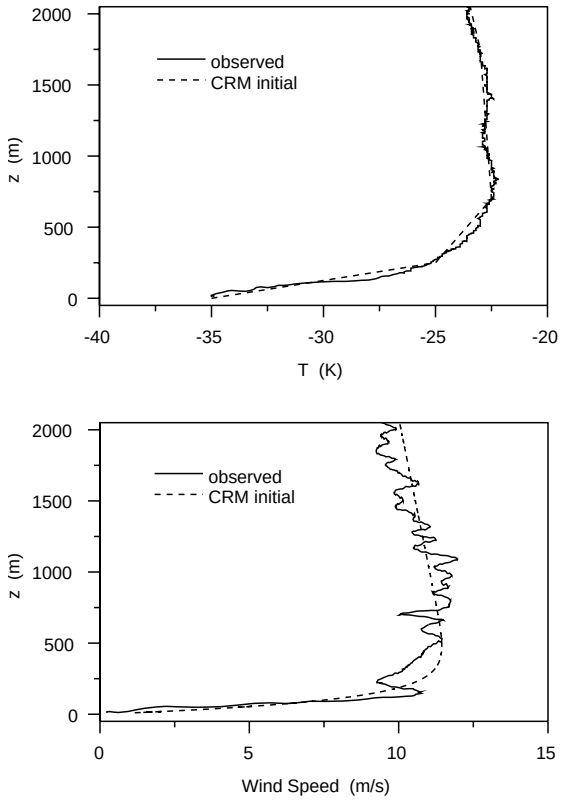

Figure 3: Observed SHEBA atmospheric profiles for Jan 18, 1998, 23:16 UTC and simplified profiles used in the CRM.

LIDAR imagery from January 20 (Figure 5), displays just such a possible sign. A low level cloud layer is observed from approximately 04:00 UTC, to 20:00 UTC. The cloud base is typically 100 to 200 m above the surface, with a thickness of up to approximately 200 m.

4. SIMULATION RESULTS

Using idealized soundings, satellite imagery, and surface data from SHEBA, a series of CRM simulations were designed and run to gauge the possible impacts of open leads on the large-scale heat and moisture budgets. The baseline simulation was of a 3.2 km lead in a 51.2 km domain, in which the lead and lead generated circulations were explicitly resolved. Other simulations examined the sensitivity to lead width, the presence of thin ice covering the lead, ambient relative humidity, and so on. Additionally, possible means of parameterizing the problem were investigated, which would allow for the impacts to be modeled without the necessity of explicitly resolving the lead (as directly resolving leads is currently impossible for large-scale models).

The first proposed method was simply to take an area weighted average of the surface fluxes as deter-

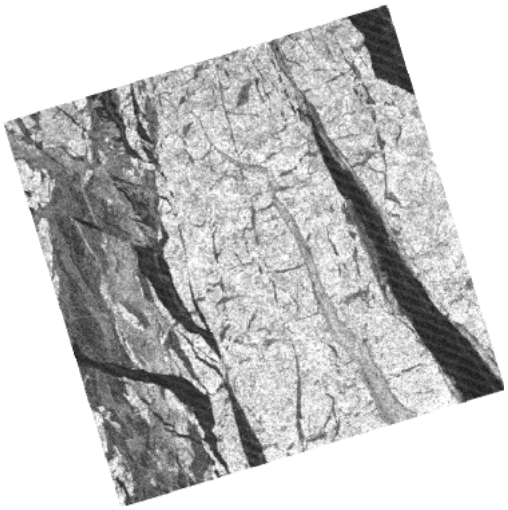

Figure 4: 60 km x 60 km SAR image from January 20, 1998 (rotated so north is at top). The ship is at center. Note the large wedge-shaped lead several km to the east.

mined over an ice surface, and over a water surface. These solutions are not coupled in any way, and no feedback exists between the over-ice fluxes and the over-water fluxes. We called this the "simple" simulation, and all feedbacks such as cloud, radiative, etc. were neglected.

The second method was a "mosaic" method. In this case a one-dimensional version of the model was used, and the applied surface flux was again a weighted average of ice and water fluxes. Unlike the "simple" case, clouds were allowed to develop, along with their attendant radiative feedbacks. The mosaic method is

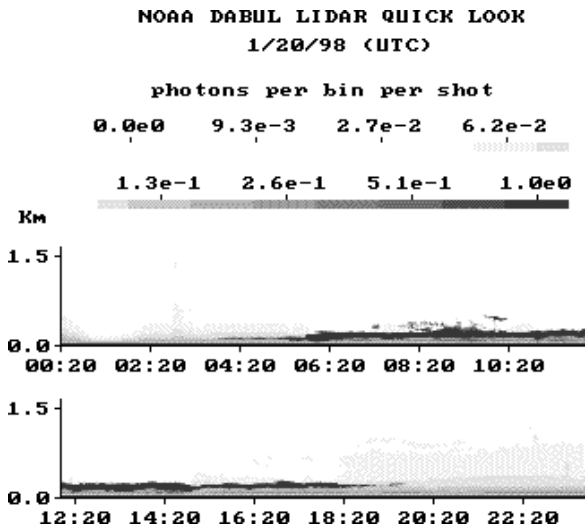

Figure 5: LIDAR imagery from the SHEBA site for January 20, 1998.

Table 1: Average surface fluxes over lead, all values in W m^{-2}.

	simple	resolved	mosaic	thin ice
S_{ld}	629	645	584	549
E_{ld}	156	158	143	79
$IR\uparrow_{ld}$	306	306	306	265
$IR\downarrow_{ld}$	140	159	143	130
net IR_{ld}	166	148	162	135
net $\uparrow$ flux	951	949	889	763

a fairly close approximation to what is used in many large-scale models.

Finally, a "thin-ice" simulation was run with a 2.5 cm layer of ice over a fully-resolved 3.2 km lead, representing a partially refrozen lead.

Table 1 summarizes the surface fluxes after two hours over the water/lead of four simulations: the "simple" parameterization, the "resolved" 3.2 km lead, the "mosaic" run, and the partially refrozen "thin ice" case. For the simple case, the absence of any lead-induced circulation or cloud feedbacks slightly reduces the sensible and latent fluxes, and increases the downward longwave when compared to the resolved lead simulation. Interestingly, the net value is quite close. The mosaic run displays significantly lower sensible and latent fluxes, due in large part to warmer near-surface air temperatures. The downward longwave flux is substantially lower, however, because of differences in the placement and temperature of the ice cloud produced by the convective plume. Finally, it is notable that the partially refrozen lead displays a proportionally much larger decrease in the latent flux when compared to the sensible heat flux. Because of this, virtually no cloud is produced, which greatly reduces the downward radiative flux over the lead.

In Table 2, we see the surface fluxes over the ice/snow surface for the same simulations. Differences here are driven primarily by variations in near surface air temperature, and placement and amount of lead-produced cloud. Since the simple case has no cloud and thus less downwelling longwave, the radiative energy

Table 2: Average surface fluxes over ice/snow, all values in W m^{-2}.

	simple	resolved	mosaic	thin ice
S_{ice}	-15	-15	-31	-17
E_{ice}	0	-1	-2	-1
$IR\uparrow_{ice}$	157	163	172	158
$IR\downarrow_{ice}$	125	137	141	125
net IR_{ice}	32	26	31	33
net $\uparrow$ flux	17	10	-2	16

Table 3: Domain averaged surface fluxes, all values in W m^{-2}.

	simple	resolved	mosaic	thin ice
S_{dom}	25	26	8	17
E_{dom}	10	9	7	4
$IR\uparrow_{dom}$	166	172	180	165
$IR\downarrow_{dom}$	126	139	141	125
net IR_{dom}	40	33	39	40
net $\uparrow$ flux	75	68	54	63

balance is quite different from the resolved case. The mosaic run displays radically different surface fluxes, largely due to considerably warmer air at the surface. The thin-ice case is actually quite similar to the simple case, as there is very little cloud to modify the radiative balance, and warmer air released by the lead only slightly affects the other fluxes.

Table 3 shows the domain averaged surface fluxes, which are essentially the area-weighted averages based on lead fraction of the data in Table 1 and Table 2. Here we can see the differing impacts upon the large-scale of the four simulations.

Lastly, as an illustration of the limitations of the mosaic method in determining the large-scale impact of leads, Figure 6 displays the vertical profiles of temperature and cloud ice. While the resolved lead case produces a penetrative plume, and an elevated cloud layer as seen in the LIDAR imagery (Figure 5), the mosaic's plume is completely ground based, and does not penetrate nearly as high. because of this, we believe that leads modeled using the mosaic method will behave quite differently, as much of the heat and moisture released by them will be quickly recaptured by the ice/snow surface.

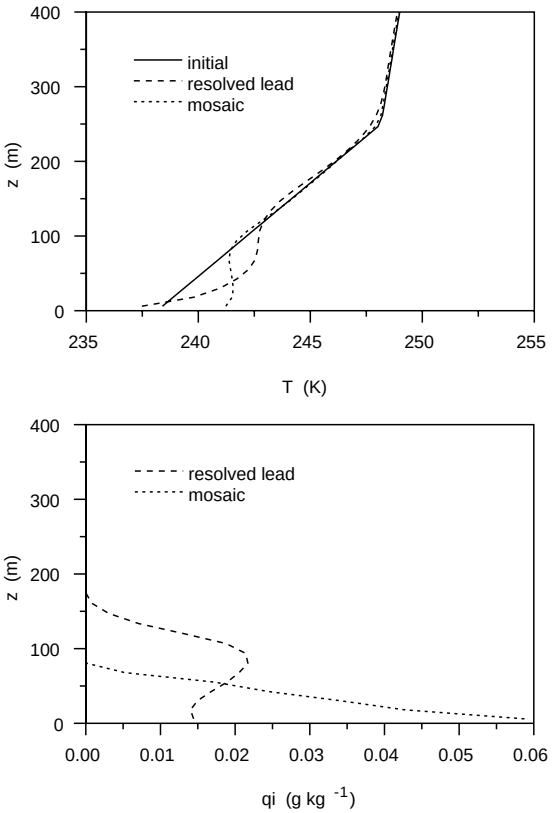

Figure 6: Domain averaged vertical profiles of temperature (K) and cloud ice (g kg^{-1}) for the resolved lead and mosaic simulations.

ACKNOWLEDGMENTS

This research was supported by NSF Grant OPP-9702583 and NASA Grant NAG-1-1718.

REFERENCES

Burk, S. D., R. W. Fett, and R. E. Englebretson, 1997: Numerical simulation of cloud plumes emanating from Arctic leads. *J. Geophys. Res.*, **102**, 16,529–16,544.

Ebert, E. E., and J. A. Curry, 1993: An intermediate one-dimensional thermodynamic sea ice model for investigating ice-atmosphere interactions. *J. Geophys. Res.*, **98**, 10,085–10,109.

Glendening, J. W., 1994: Dependence of a plume heat budget upon lateral advection. *J. Atmos. Sci.*, **51**, 3517–3530.

Intrieri, J., 1999: SHEBA: LIDAR, ETL DABUL System; Quick-look PRELIMINARY data from Ice Camp. `http://www.joss.ucar.edu/cgi-bin/codiac/dss?13.302`.

Krueger, S. K., G. T. McLean, and Q. Fu, 1995: Numerical simulation of the stratus to cumulus transition in the subtropical marine boundary layer: I: Boundary layer structure. *J. Atmos. Sci.*, **52**, 2839–2850.

Moritz, R. E., 1999: Soundings, PRELIM Ice Camp NCAR/GLAS raobs (ASCII). `http://www.joss.ucar.edu/cgi-bin/codiac/dss?13.202`.

Pinto, J. O., and J. A. Curry, 1995: Atmospheric convective plumes emanating from leads. Part 2: Microphysical and radiative processes. *J. Geophys. Res.*, **100**, 4633–4642.

RADARSAT SAR Images of SHEBA, Copyright ©1998 by Canadian Space Agency: distributed by H. Stern. `http://psc.apl.washington.edu/Harry/Radarsat/`, SAR imagery processed at the Alaska SAR Facility (Fairbanks) and distributed through the SHEBA Project Office (Seattle).